This is an Accepted Manuscript of an article published by Taylor & Francis in **ULTRASTRUCTURAL PATHOLOGY** on 07.04.2020, available online: https://www.tandfonline.com/doi/abs/10.1080/01913123.2020.1744784?journalCode=iusp20

Postprint of: Tretiakow D., Skorek A., Ryl J., Wysocka J., Darowicki K., Ultrastructural analysis of the submandibular sialoliths: Raman spectroscopy and electron back-scatter studies, Ultrastructural Pathology, vol. 44, nr 2 (2020), DOI: 10.1080/01913123.2020.1744784

Ultrastructural analysis of the submandibular sialoliths: Raman spectroscopy and electron back-scatter studies.

Dmitry Tretiakow[1], Andrzej Skorek[1], Jacek Ryl[2], Joanna Wysocka[2], Kazimierz Darowicki[2]

[1] Department of Otolaryngology, Medical University of Gdansk, Poland

[2] Department of Electrochemistry, Corrosion and Materials Engineering, Gdansk University of Technology, Poland

Corresponding author:
Dmitry Tretiakow
Department of Otolaryngology, Medical University of Gdansk
Ul. Smoluchowskiego 17, 80-214 Gdańsk
tel. +4858 349 3110 d.tret@gumed.edu.pl

Sources of support in the form of grants: This work was supported by departmental funding of the Faculty of Medicine (Medical University of Gdansk) and Faculty of Chemistry (Gdansk University of Technology).

Abstract

Introduction: The aim of work was the epidemiological analysis of the occurrence of sialolithiasis of the submandibular gland in adults and the evaluation of the ultrastructure of salivary stones.

Methods: The study sample consisted of 44 sialoliths. Analysis of the structure and chemical composition of sialoliths was performed using a Scanning Electron Microscope and Raman Spectroscopy.

Results: Comparing our results with the literature we can say that the epidemiology of sialolithiasis has not changed significantly over the past 50 years. A wide variety of sialoliths structure was observed. In 75% (33) cases a layered structure of salivary stones was observed, while in 25% (11) - homogeneous structure. The various distribution of organic and inorganic components was observed among all the analyzed sialoliths.

Conclusion: Raman spectroscopy allows for preliminary analysis of the sialoliths structure with only a qualitative assessment of their composition, which significantly reduces the research value of this method. The presence of organic and inorganic compounds in the core and inner layers of the salivary glands stones confirms 2 basic theories of the formation of sialoliths: inflammation and deposition of the inorganic component as a result of disruption of saliva flow in the salivary glands.

Keywords: salivary diagnostics, scanning electron microscopy, saliva, infrared spectroscopy, calculus, inflammation.

Introduction

Sialolithiasis is one of the causes of salivary gland inflammation that is characterized by the formation of single or multiple deposits (sialoliths) in the salivary ducts or salivary glands. The resulting salivary duct obstruction inhibits the saliva flow, which in turn leads to inflammation of the salivary gland. The most common symptoms of sialolithiasis are of salivary gland swelling and pain (intensified during a meal) and fever [1–4].

The incidence of sialolithiasis is about 2.9-5.5 cases per 100,000 and most cases occur in the 30-50 years of age group [2,3,5]. Salivary gland stone can be located in the salivary gland duct or the salivary gland parenchyma. In most cases, the stones are located in the submandibular glands (about 80-85%), whereas the rest are found in the parotid salivary glands (15-20%) [2,3,6–8]. The high incidence of sialolithiasis of the submandibular gland is the reason that almost all literature is focused on stones obtained from the submandibular glands.

Although several factors predisposing to sialolith formation are already known, the cause of sialolith formation is still not entirely clear. Thus there are no specific and effective ways to prevent sialoliths [5,8–14]. An important predisposing factor for precipitation may be an increased concentration of calcium in the saliva together with a reduced concentration of crystallization inhibitors (e.g. inositol phosphate - $C_6H_{15}O_{15}P_3$) [9,15]. Smoking and increased sodium levels in saliva both increase the risk of salivary stone formation [16].

Conservative treatment methods have poor effectiveness and tend to be used only in cases of very small sialoliths (<4 mm) [4,8,17,18]. Surgical treatment is almost always indicated, which often requires general anesthesia and carries the risk of complications such as facial (marginal mandibular branch), sublingual and lingual nerve palsy [3,6,19–22].

The first results of research on the structure of salivary gland stones were published at the end of the 20th century [23,24]. Sialolith is a calcified solid mass, consisting mainly of organic material in its central part, surrounded by inorganic layers, arranged concentrically or irregularly, with varying degrees of mineralization. Inorganic components are primarily calcium and phosphates in the form of hydroxyapatite ($Ca_{10}(PO_4)_6(OH)_2$, magnesium whitlockite ($Ca_9MgH(PO_4)_7$ and brushite ($CaHPO_4{\cdot}2H_2O$. [4,5,9,15,25–28]. High sulphur content indicates that the organic matter in the sialoliths corresponds to degenerated and condensed secretory material [29].

Due to the scarce and controversial literature data about the etiopathogenesis of sialolith formation and prevention, we attempted a detailed layered analysis of the structure of sialoliths obtained from submandibular gland ducts. We aimed to contribute to further research in the

search for methods to prevent the development of sialolithiasis and the possibility of conservative treatment.

Material and Methods

The study was carried out on samples of 44 salivary sialoliths obtained from the submandibular gland duct from 44 patients with submandibular sialolithiasis treated at the Otolaryngology Department of the Medical University of Gdansk during conventional surgical treatment in the period January 2019-September 2019. Specimens were kept dry in medical containers.

The exemplary micrographs were made using a Scanning Electron Microscope (SEM), operating with a variable pressure chamber at a pressure of 90 Pa to minimize ionization of the specimen. A back-scatter electron (BSE) detector was used for the analysis. The accelerating voltage was 20 kV. There were no pre-treatment procedures applied besides cutting the investigated salivary stones to reveal their core.

Spectroscopy studies were carried out using a Raman confocal microscope (Horiba LabRAM ARAMIS, Japan). Spectra were recorded in a range of 200–4000 cm^{-1}, using a 532 nm diode-pumped 30 mW solid-state (DPSS) laser in combination with a 10x objective magnification and 50 µm confocal aperture. The diffraction grating was 1200 slits/mm. Optical filter d0.6 was used during the measurements. Each spectrum was recorded in at least three replicated with an exposure time of 20 s. The laser source was calibrated versus silicon at 519 cm^{-1}. The study protocol was approved by the local Hospital Ethical Committee.

Results

Epidemiological analysis

The obtained salivary stones were different in size and shape, ranging between few and even several dozen millimeters. Stones differed in color, which most often presented various shades of white and yellow (Tab. 1).

The analyzed deposits were divided into 4 groups according to the classification of salivary gland stones described by Lustmann et al. [8] (Tab. 2). The stones were further

classified by maximum diameter as per Lustmann et al. (group I: 1–5 mm; group II: 6–10 mm; group III: 11–15 mm; group IV: >15 mm).

Raman spectroscopy in the analysis of sialolith structure.

Raman spectroscopy studies were performed to determine the chemical composition of the sialoliths. Raman spectroscopy measurements were obtained for each of the investigated salivary stones, Graph. 1 illustrates the results obtained for 4 randomly chosen sialoliths.

It is important to note that the Raman spectroscopy provides primarily qualitative information, while the quantitative analysis is hindered.

Scanning Electron Microscope (SEM) in the analysis of the sialoliths structure.

We used the SEM method for the initial analysis of the sialoliths', and collected over 600 micrographs of the specimens.

For the initial analysis of the structure of salivary gland stones, we used the SEM method. During the tests, we took over 600 photos of salivary stones specimens. The SEM-BSE micrographs for the selected specimens are presented in Figure 1a-i. The utilization of BSE detector allows to compare of local areas of the different chemical composition since the probability of electron back-scatter event is proportional to the atomic mass of the analyzed material. Thus, the bright areas on the micrographs are composed of heavier elements.

It is clearly visible, that the chemical constitution of the analyzed stones varies from one to another. Some of the stones are quite homogeneous (Fig. 1b,e,i), which is manifested by small local differences on the histogram of SEM-BSE micrograph and visible only at high magnifications (in the inset). On the other hand, the layered nature of the most specimens are clearly highlighted (Fig. 1a,f,g,h).

Interestingly, one can see further visual discrepancies in the volume chemistry of these layered stones. The layered, heterogeneous nature of certain sialoliths was highlighted by arrows placed on Graph. 1. In the most cases of stones with layered structure, the organic phase forms the interlayer (marked with the bright green arrows on Fig. 1a,f,g,h), however, in the very few cases of organic sialolith core, the interlayer may be built of limestone structure, such as hydroxyapatite (red arrows on Fig. 1d). The most outer layers of the largest stones appear under the SEM-BSE imaging in significantly brighter colors, suggesting they are built of heavier elements (Fig. 1a,h,e).

It is important to note, that the most homogeneous stones discussed earlier are similar in color and structure, merely lacking the heterogeneous organic-heavy ring. Some of the smaller, yet heterogeneous salivary stone specimens contain a significantly lower amount of heavy elements, see Fig. 1c,d. It was also observed, that the discussed type of stones is significantly more dense, often possessing voids in their structure.

Discussion

Epidemiological analysis

Our results of epidemiological date analysis are very similar to the literature data on sialolithiasis of the submandibular gland. Within the study population described by Yiu et al. [16], there were 56 men (95%) and three women (5%). The median age of the cohort was 58 years (range 25–89 years). Within the cohort, 45 patients (76%) had one stone and 14 patients (24%) had more than one stone. Salivary stones were found in the left submandibular gland in 18 patients (37%) and the right submandibular gland in 28 patients (57%); three patients (6%) had bilateral disease. Sigismund et al.[18] described in their review a group consisting of 977 males (53.3%) and 856 females (46,7%), average age 42.5 years (6–91) and average stones size 8.3 mm (0.1–35). The next review included an analysis of the 245 patients [8], 121 (49.4%) were male and 124 (50.6%) female. Patients ranged between 6 and 94 years of age, with an almost even incidence in the 3rd to 6th decades of life (18.4%, 18.8%, 17.6%, 15.5% respectively). Distribution between the right (50.2%) and left (47.7%) sides of the affected glands also were almost equal, and 3 cases (1.2%) had bilateral involvement.

The mean size of the sialoliths in our study group (9.5-11mm) is comparable to the results described in a large review by Sigismund et al. [18], where the average diameter of submandibular sialoliths was 8.3 mm (range 1–35 mm). A similar, as in the aforementioned review, distribution by group according to the Lustmann classification was observed when analyzing our results (Fig. 1). A total of 1,367 calculi in the submandibular gland were classified, as per Lustmann et al.: 46% of stones were in group II, 30% were in group I, 17% were in group III, and 6% were in group IV.

As for the shape of the stones analyzed, in our study we observed symmetrical (n=7 (16%) and asymmetrical sialoliths (n=37 (84%). According to Im et al.[30] the cross-section of the specimen showed asymmetric width and color pattern of the outer shell.

According to our data, in the study group 12 (27%) patients had a history of smoking and 10 (23%) were active smokers. In comparison, Yiu et al.[16] described 35 patients (59%) with a smoking history and 16 (27%) reported as current smokers.

Raman spectroscopy in the analysis of sialolith structure.

In some of the published studies the sialolith specimens were embedded in epoxy resin, followed by cross-cutting into 2 pieces by using a precision diamond cutter and polishing using SiC polishing papers (#600) and alumina powder (diameter of 0.3 mm) [30]. Authors decided not to use this approach however, to avoid sample surface contamination, particularly with carbon, since the applied techniques are surface-sensitive.

Moreover, the obtained results did not allow for a clear distinction of various chemical components. Furthermore, the characteristic peaks were observed regardless of the studied specimen, thus suggesting a similar origin of all the stones. The analysis confirmed that the studied sialoliths consisted of both organic (Raman shift at 2000-3500 cm^{-1}) and inorganic (200-1500 cm^{-1}) phases. We also noted some artefacts (noise and overlapping bands), related to the complex nature and large chemical diversity of studied materials. Similar observations were reported in several studies of sialoliths from both major and minor salivary glands [24,29,31,32].

Each observed peak was assigned to the type of corresponding chemical bonds. The analysis confirmed the presence of the following organic compounds: collagen, glycoproteins, amino acids, carbohydrates. The inorganic compounds were hydroxyapatite $3Ca_3(PO_4)_2 \cdot Ca(OH)_2$, calcium phosphate $Ca_3(PO_4)_2$ and/or magnesium phosphate $Mg_3(PO_4)_2$, calcium carbonate $CaCO_3$ and others (see Table 2).

Similar results are also described by other authors. The powder and single-crystal electron diffraction patterns demonstrated that Ca- and P-based electrolytes tended to crystallize in a hexagonal crystal structure close to that of hydroxyapatite. The presence of Mg in the mineralized regions suggests the formation of whitlockite, although the phase has a minor presence and could not be detected by the powder and single-crystal electron diffraction experiments [29,31]. The study demonstrates that hydroxyapatite is not at all the main constituent, the majority of them are constructed with other apatites, among them are amorphous carbonated calcium phosphate and carbonated apatite and whitlockite. The inner part of sialoliths is thinly stratified by apatites and/or proteins according to their history of creation and their growth [32].

Nolasco et al.[29] stated that a high sulphur content indicates that the organic matter in the sialoliths corresponds essentially to degenerated and condensed secretory material. We did not detect sulphur in our sample using Raman spectroscopy.

Scanning Electron Microscope (SEM) in the analysis of the sialoliths structure.

SEM observation of the specimens revealed several types depending on their organization: concentric (Fig. 1g,h) versus irregular (Fig. 1c,d), a high degree of mineralization (Fig. 1e,i) versus low (Fig. 1d). Nolasco et al. [29] had similar observations. In contrast to their study, we can distinguish other types of sialoliths according to their structure: (homogenous (Fig. 1e,i) versus layered (Fig. 1a,h).

According to the research by Riesco et al.[26], Im et al. [30] and Jensen et al. [23] sialoliths may have various shapes and structures, while some salivary gland stones may consist of the organic core with a surrounding organic and mixed, concentric laminated or irregular structures, such as observed in Fig. 1c,d. A similar observation was confirmed by Szalma [33] and Sabot [32]. While these stones are sometimes appearing, our study shows the majority of sialoliths have a greater degree of calcification at the periphery than in the spinal area.

The conclusion regarding the largest sialoliths being built with a higher amount of the limestones in their composition is in good agreement with Raman spectroscopy studies, suggesting these stones have a higher share of hydroxyapatite, as well as other inorganic compounds: phosphates, carbonates and others. The intermediate layer of the aforementioned stones is the most often dominated by less heavy compounds, most likely organic in nature, as highlighted with green arrows on Fig. 1. The ring formed by these compounds is loosely attached to the core, often leading to adhesive delamination when the specimens were cut.

We observed that 27 sialoliths of 41 in total were larger than 6 mm and composed of inorganic structures, but this is not unequivocal. Jensen et al. suggest that minor salivary gland calculi arise as a result of the accumulation of organic material in a duct: this material is eventually transformed into a resinous mass; mineral salts are usually, but not always, deposited in the matrix; growth occurs by the addition of concentric layers of organic material. Also, the irregular distribution, amount, and pattern of mineralized material in the matrix suggest that in most case mineralization occurs in a noncyclic fashion [23]. In some cases, we observe a similar situation, but not exclusively, but only as part of the sialoliths, which confirms the theory of sialoliths' formation described above.

Grases et al. [9] described the stones which contain a substantial amount of organic matter both on their outer surface and inside the stone. Hydroxyapatite spheres are largely

accumulated in stone cavities as either individual entities or agglomerates. In this publication, we met the description some sialoliths are exclusively composed of organic materials, but in our study, we did not encounter this type of salivary gland stones. We observed sialoliths with organic layers domination (Fig. 1d,g).

In the majority of sialoliths, i.e. 37 (84%), we found the presence of a core that was surrounded by concentric or irregular patterns with variable degrees of mineralization. Similar observations reported by other researchers [29,34,35].

In our study, we did not find bacterial features in sialoliths as it was described by Nolasco et al. [29]. We agree that the organic fraction observed under the microscope consists largely of organic material, i.e. proteins, DNA, peptides, etc. which is the basic of bacteria organelle. Deposits observed by the authors of the publications may, therefore, constitute agglomerates of bacterial colonies, however, that SEM / EDS techniques do not allow for an unequivocal determination as to which organic substances it is dealing with. Bacteriological verification by the authors of the article was not performed.

As in the case of kidney stones, expanding knowledge about the structure of sialoliths should lead to further development of new preventive, diagnostic and patient-tailored treatment methods of patients with sialolithiasis [36,37]. Examination of kidney stones in the past and the highlighting of a number of their types: calcium-containing stones, struvite stones, uric acid stones, and several other rare types has enabled the development of diagnostic methods and an individual approach in the treatment of patients with different types of kidney stones [38,39].

Conclusions

Epidemiology of sialolithiasis has not changed significantly over the past 50 years. A similar frequency of sialolithiasis of the submandibular gland is observed regardless of age and sex. This observation suggests that eating habits and food quality have less effect on the formation of salivary gland stones relative to other known predisposing factors.

Raman spectroscopy is a method often used in the study of salivary gland stones. It allows for the preliminary analysis of the structure of sialoliths with a qualitative but not quantitative assessment of their composition. It can be considered that this method offers very limited opportunities to expand knowledge of the structure of salivary glands and it is not suitable for further study of salivary gland stones to expand knowledge of their structure.

SEM microscopy in the back-scattered electron (BSE) mode allows imaging and explicit differentiation of the salivary stone phases. Based on SEM, we noticed that despite the existing sialoliths divisions, the analyzed salivary stones can also be divided into inorganic and mixed type. This may be useful in further research into their structure and cause rise and development, and contribute to establishing a classification of sialoliths in the future.

SEM observation of the specimens revealed several types depending on their organization: concentric versus irregular, a high degree of mineralization versus low. The diversity of the sialoliths structure may explain the mechanical strength of sialoliths and their insolubility in salivary ducts.

As in the case of kidney stones, expanding knowledge about the structure of sialoliths should lead to further development of new preventive, diagnostic and patient-tailored treatment methods of patients with sialolithiasis.

Acknowledgments

This work was supported by departmental funding of the Faculty of Medicine (Medical University of Gdansk) and Faculty of Chemistry (Gdansk University of Technology).

The study protocol was approved by the Regional Bioethics Committee of Gdansk Medical University, Poland (approval nr. NKBBN/452/2019).

The authors declare no potential conflicts of interest concerning the authorship and/or publication of this article.

All authors gave final approval and agree to be accountable for all aspects of the work.

All authors contributed equally to this work.

Author contributions:

D. Tretiakow: obtaining material samples, contributed to the study concept, design, data analysis, and interpretation, drafted the manuscript, gave final approval.

A. Skorek: obtaining material samples, contributed to the study concept and design, critically revised the manuscript, gave final approval.

J. Ryl: contributed to design, data acquisition (SEM), analysis and interpretation, design, drafting the manuscript, gave final approval.

J. Wysocka: data acquisition (Raman spectroscopy), analysis and interpretation, drafted manuscript, gave final approval.

K. Darowicki: contributed to the conception, critically revised the manuscript, gave final approval.

References

1. Hunt T, Bowyer D. Reinjection and gravity changes at Rotokawa geothermal field, New Zealand. Geothermics. 2007 Oct;36(5):421–35.
2. Delli K, Spijkervet FKL, Vissink A. Salivary gland diseases: infections, sialolithiasis and mucoceles. Monogr Oral Sci. 2014;24:135–48.
3. Escudier M, McGurk M. Symptomatic sialoadenitis and sialolithiasis in the English population, an estimate of the cost of hospital treatment. Br Dent J. 1999 May 8;186(9):463–6.
4. Trujillo O, Drusin MA, Rahmati R. Rapid recurrent sialolithiasis: Altered stone composition and potential factors for recurrence. Laryngoscope. 2017;127(6):1365–8.
5. Schroder SA, Homoe P, Wagner N, Bardow A. Does saliva composition affect the formation of sialolithiasis? J Laryngol Otol. 2017;131(2):162–7.
6. Zenk J, Koch M, Klintworth N, König B, Konz K, Gillespie MB, et al. Sialendoscopy in the diagnosis and treatment of sialolithiasis: A study on more than 1000 patients. Otolaryngol - Head Neck Surg (United States). 2012;147(5):858–63.
7. Chang JL. Salivary Gland Imaging. In: Gland-Preserving Salivary Surgery. Cham: Springer International Publishing; 2018. p. 15–26.
8. Lustmann J, Regev E, Melamed Y. Sialolithiasis. A survey on 245 patients and a review of the literature. Int J Oral Maxillofac Surg. 1990 Jun;19(3):135–8.
9. Grases F, Santiago C, Simonet BM, Costa-Bauzá A. Sialolithiasis: Mechanism of calculi formation and etiologic factors. Clin Chim Acta. 2003;334(1–2):131–6.
10. Marchal F, Kurt A-M, Dulguerov P, Lehmann W. Retrograde Theory in Sialolithiasis Formation. Arch Otolaryngol Neck Surg. 2001 Jan 1;127(1):66.
11. Williams MF. Sialolithiasis. Otolaryngol Clin North Am. 1999 Oct;32(5):819–34.
12. Huoh KC, Eisele DW. Etiologic Factors in Sialolithiasis. Otolaryngol Neck Surg. 2011 Dec 13;145(6):935–9.
13. Pradeep AR, Agarwal E, Arjun Raju P, Rao MSN, Faizuddin M. Study of Orthophosphate, Pyrophosphate, and Pyrophosphatase in Saliva With Reference to

Calculus Formation and Inhibition. J Periodontol. 2011;82(3):445–51.

14. Li W, Wei L, Wang F, Peng S, Cheng Y, Li B. An experimental chronic obstructive sialadenitis model by partial ligation of the submandibular duct characterised by sialography, histology, and transmission electron microscopy. J Oral Rehabil. 2018;45(12):983–9.
15. Stelmach R, Pawłowski M, Klimek L, Janas A. Biochemical structure, symptoms, location and treatment of sialoliths. J Dent Sci. 2016 Sep;11(3):299–303.
16. Yiu AJ, Kalejaiye A, Amdur RL, Todd Hesham HN, Bandyopadhyay BC. Association of serum electrolytes and smoking with salivary gland stone formation. Int J Oral Maxillofac Surg. 2016;45(6):764–8.
17. Capaccio P, Torretta S, Ottavian F, Sambataro G, Pignataro L. Modern management of obstructive salivary diseases. Acta Otorhinolaryngol Ital. 2007 Aug;27(4):161–72.
18. Sigismund PE, Zenk J, Koch M, Schapher M, Rudes M, Iro H. Nearly 3,000 salivary stones: Some clinical and epidemiologic aspects. Laryngoscope. 2015;125(8):1879–82.
19. Kopeć T, Wierzbicka M, Szyfter W, Leszczyńska M. Algorithm changes in treatment of submandibular gland sialolithiasis. Eur Arch Oto-Rhino-Laryngology. 2013;270(7):2089–93.
20. Sun Y-T, Lee K-S, Hung S-H, Su C-H. Sialendoscopy With Holmium:YAG Laser Treatment for Multiple Large Sialolithiases of the Wharton Duct: A Case Report and Literature Review. J Oral Maxillofac Surg. 2014 Dec;72(12):2491–6.
21. Kraaij S, Karagozoglu KH, Forouzanfar T, Veerman ECI, Brand HS. Salivary stones: symptoms, aetiology, biochemical composition and treatment. Br Dent J. 2014 Dec 5;217(11):E23–E23.
22. Zenk J, Koch M, Iro H. Extracorporeal and Intracorporeal Lithotripsy of Salivary Gland Stones: Basic Investigations. Otolaryngol Clin North Am. 2009 Dec;42(6):1115–37.
23. Jensen JL, Howell F V., Rick GM, Correll RW. Minor salivary gland calculi. Oral Surgery, Oral Med Oral Pathol. 1979 Jan;47(1):44–50.
24. Anneroth G, Hansen LS. Minor salivary gland calculi. A clinical and histopathological study of 49 cases. Int J Oral Surg. 1983 Apr;12(2):80–9.
25. Su Y, Zhang K, Ke Z, Zheng G, Chu M, Liao G. Increased calcium and decreased magnesium and citrate concentrations of submandibular/sublingual saliva in sialolithiasis. Arch Oral Biol. 2010 Jan;55(1):15–20.
26. Riesco JM, Juanes JA, Díaz-González MP, Blanco EJ, Riesco-López JM, Vázquez R. Crystalloid architecture of a sialolith in a minor salivary gland. J Oral Pathol Med. 1999

Nov;28(10):451–5.

27. Durbec M, Dinkel E, Vigier S, Disant F, Marchal F, Faure F. Thulium-YAG laser sialendoscopy for parotid and submandibular sialolithiasis. Lasers Surg Med. 2012 Dec;44(10):783–6.
28. Su Y xiong, Zhang K, Ke Z fu, Zheng G sen, Chu M, Liao G qing. Increased calcium and decreased magnesium and citrate concentrations of submandibular/sublingual saliva in sialolithiasis. Arch Oral Biol. 2010;55(1):15–20.
29. Nolasco P, Anjos AJ, Marques JMA, Cabrita F, da Costa EC, Maurício A, et al. Structure and Growth of Sialoliths: Computed Microtomography and Electron Microscopy Investigation of 30 Specimens. Microsc Microanal. 2013 Oct 4;19(5):1190–203.
30. Im YG, Kook MS, Kim BG, Kim JH, Park YJ, Song HJ. Characterization of a submandibular gland sialolith: micromorphology, crystalline structure, and chemical compositions. Oral Surg Oral Med Oral Pathol Oral Radiol. 2017;124(1):e13–20.
31. Sakae T, Yamamoto H, Hirai G. Mode of Occurrence of Brushite and Whitlockite in a Sialolith. J Dent Res. 1981 Apr 8;60(4):842–4.
32. Sabot J-F, Gustin M-P, Delahougue K, Faure F, Machon C, Hartmann D-J. Analytical investigation of salivary calculi, by mid-infrared spectroscopy. Analyst. 2012;137(9):2095.
33. Szalma J, Böddi K, Lempel E, Sieroslawska AF, Szabó Z, Harfouche R, et al. Proteomic and scanning electron microscopic analysis of submandibular sialoliths. Clin Oral Investig. 2013 Sep 27;17(7):1709–17.
34. Ostwald W. Zur Theorie der Liesegang'schen Ringe. Kolloid-Zeitschrift. 1925;
35. Epivatianos A, Harrison JD, Dimitriou T. Ultrastructural and histochemical observations on microcalculi in chronic submandibular sialadenitis. J Oral Pathol Med. 1987 Nov;16(10):514–7.
36. Mayans L. Nephrolithiasis. Prim Care Clin Off Pract. 2019 Jun;46(2):203–12.
37. Pfau A, Knauf F. Update on Nephrolithiasis: Core Curriculum 2016. Am J Kidney Dis. 2016 Dec;68(6):973–85.
38. Moe OW. Kidney stones: pathophysiology and medical management. Lancet. 2006 Jan;367(9507):333–44.
39. Sakhaee K, Maalouf NM, Sinnott B. Kidney Stones 2012: Pathogenesis, Diagnosis, and Management. J Clin Endocrinol Metab. 2012 Jun 1;97(6):1847–60.

Figure/table legend:

Table 1. Patient demographics, including the number, type and size of sialoliths.

Table 2. The location of characteristic bands found on Raman spectra of the investigated sialoliths with corresponding chemical bonds.

Table 3. Maximum diameters of sialoliths in our sample (classification suggested by Lustmann et al).

Graphic 1. Raman spectra obtained for 4 randomly selected representative salivary stones from our sample.

Figure 1. The SEM-BSE micrographs of the exemplary analysed salivary stones.

Table 1 Patient demographics, including the number, type and size of sialoliths.

	N	**Average (years)**	**Side**	**Type of stones**	**Size (mm)**
Men	20 (45%)	45,5 (32-59)	left - 13 right - 7	layer - 14 homogeneous - 6	9,5 (4-15)
Women	24 (55%)	49 (35-63)	left - 14 right - 10	layer - 19 homogeneous - 5	11 (5-17)

Table 2 The location of characteristic bands found on Raman spectra of the investigated sialoliths with corresponding chemical bonds.

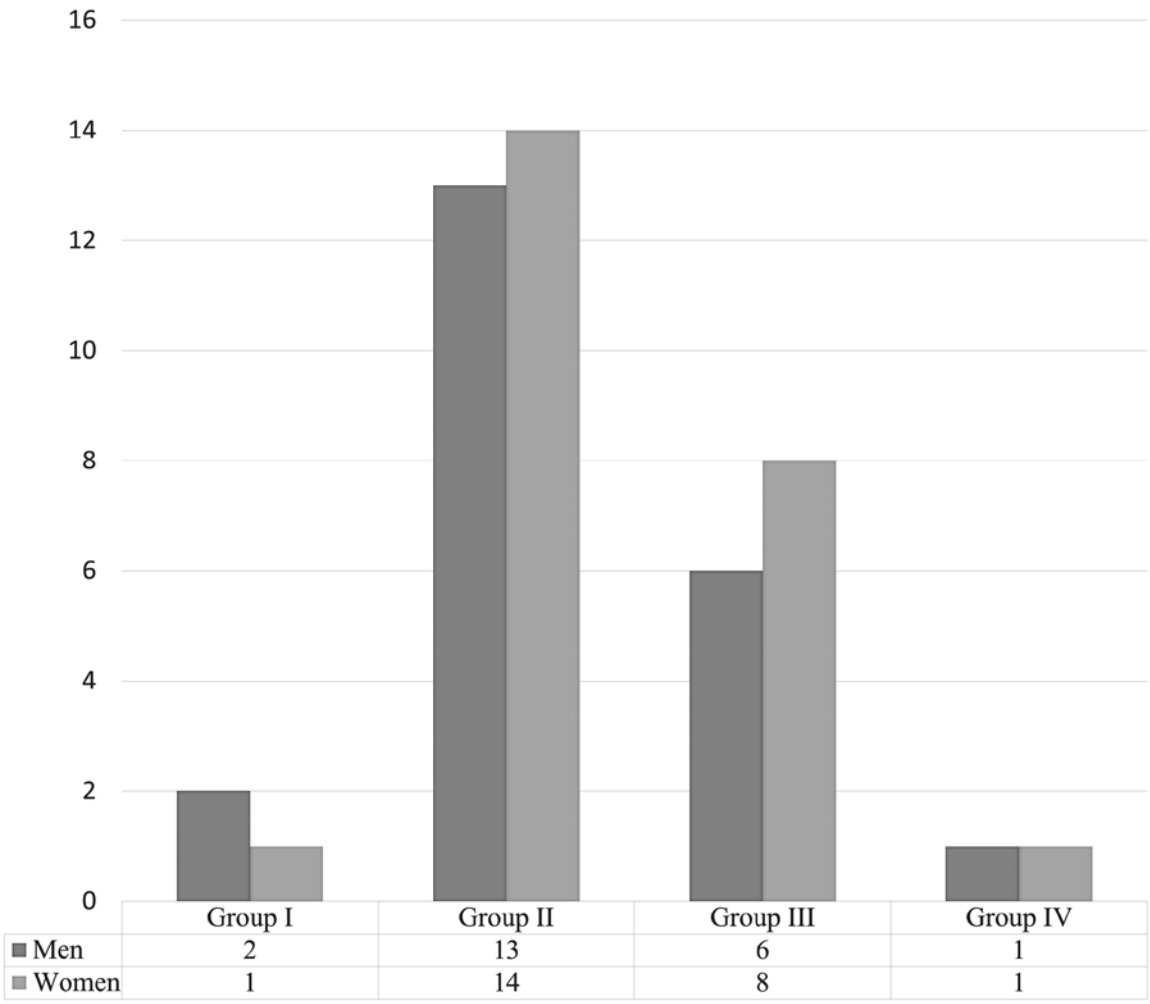

	Group I	Group II	Group III	Group IV
Men	2	13	6	1
Women	1	14	8	1

Table 3. Maximum diameters of sialoliths in our sample (classification suggested by Lustmann et al).

Band shift [cm^{-1}]	**Type of chemical bond**
200.0	$CaHPO_4$
233.0	$CaHPO_4$, OH···O
292.3	C – C
372.0	O – P – O
459.7	O – P – O, PO_4^{3-}
583.9	PO_4^{3-}
733.1, 776.4	CO_3^{2-}
837.9	C – CH, C – OH, O – CH
942.7	PO_4^{3-}, P – O(H)
1132.9	CO_3^{2-}, PO_4^{3-},C – C
1251.4	P = O, P – OH, $–CH_2$,CH_2 – OH
1429.1	$–CH_2$, C – O
1453.0, 1479.2, 1633.0	C – O
1756.0	C = O
2833.6	$=CH_2$
3070.5, 3117.2, 3489.7, 3515.9, 3580.8	O – H

Figure 1. The SEM-BSE micrographs of the exemplary analysed salivary stones.

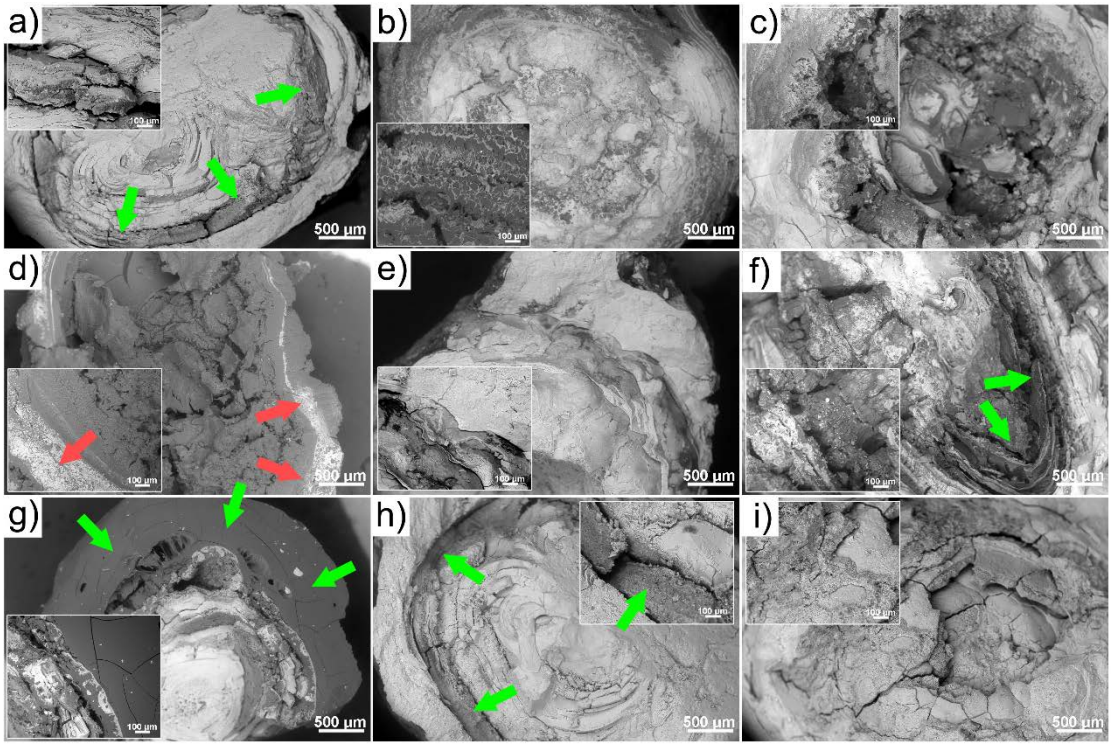

Graphic 1. Raman spectra obtained for 4 randomly selected representative salivary stones from our sample.